PROCEEDINGS of the
23rd International Congress on Acoustics
9 to 13 September 2019 in Aachen, Germany

A theory for stethoscope acoustics

Maximilian NUSSBAUMER[(1)], Leyre TROYAS-MARTINEZ[(2)], Anurag AGARWAL[(3)]

[(1)]University of Cambridge, United Kingdom, mn406@cam.ac.uk
[(2)]University of Cambridge, United Kingdom, lt397@alumni.cam.ac.uk
[(3)]University of Cambridge, United Kingdom, anurag.agarwal@eng.cam.ac.uk

Abstract
Maximising the signal to noise ratio while considering ergonomics and aesthetics is the key design challenge for modern stethoscopes. In order to optimise the design, there is a need for a well-validated model for the transfer function from a source within the chest to the output signal obtained. Most variants of the stethoscope are air-coupled sensors. Here we propose a new theory for the acoustics of this type of sensor, which takes into account the coupling between the sensor and the human chest. We have conducted rigorous experiments to characterise the transfer function of the chest-stethoscope system and have investigated the effects of key design parameters. Our data confirms traditional findings on the effects of bell geometry and diaphragm usage, but also highlights the importance of the coupling between the sensor and the chest, and reveals features of the transfer function that are not captured by existing models. Our model employs a transmission matrix formulation and discretises the system into lumped element components. It can be used to inform design choices for acoustic, electronic and dual-mode stethoscopes, opening up the possibility of an optimum design that maximises the signal to noise ratio for a desired application.

Keywords: Stethoscope, Lumped-Element, Coupling

1 INTRODUCTION

It has long been known that biological sounds from the heart and lungs convey useful diagnostic information. The initial stethoscope, invented just over 200 years ago by the French physician René Laennec, was a simple cylinder in which the enclosed air coupled the chest to the ears of the physician. Over two hundred years later, air-coupled sensors are still the predominant method of listening to and recording body sounds.

Despite their ubiquitous use, there is no simple or standardised way to compare stethoscopes or evaluate new designs. This is largely due to the fact that an evaluation of the standalone acoustic properties of the stethoscope (as performed e.g. by Abella et al. [1]) is insufficient in assessing its performance when coupled to the human body. This is because the application of a stethoscope modifies the vibration of the chest surface.

Over the years many researchers have carried out experiments to compare sets of stethoscopes [1] [2]. Unfortunately is is difficult to compare results across studies because the properties of the coupling between the sensor and the chest are difficult to control and quantify. One approach has been to carry out experiments using the sensors directly on human subjects [2] [3]. The issue here is that there is no way to accurately control the input signal, or for other researchers to replicate the exact physical properties of the test subject. Another approach is to use an experimental rig built to mimic the human chest (commonly referred to as a 'phantom' [4]). In this case it is possible to measure an input signal (although it is still fairly arbitrary as to how and where this should be defined). Kraman et al. [5] and Mansy et al. [4] have both carried out extensive research on optimising the design of chest phantoms, however neither group's testing system has been adopted by the wider research community.

Nowak and Nowak [3] argue that any attempt to use a phantom in testing stethoscopes will fail to accurately replicate the stethoscope's use in a diagnostic situation. Their preferred approach is to collect data on a large number of human subjects and use statistical methods to account for variations in input signal.

Beyond experimental comparisons between stethoscopes, it is of interest to develop a physical understanding of how these systems work. Perhaps the most complete attempt at discussing the physics of air-coupled sensors can be found in the chapter on "Sensing by Acoustic Biosignals" by Kaniusas [6]. Kaniusas makes extensive use of early research by Ertel [7] and others to discuss the resonant properties of various sub-systems of the coupled chest-sensor system. In doing so it is possible to make qualitative statements about how changes in design parameters may affect the overall response. However, a combined model for the coupled system is not presented.

The most complete attempts to model the coupled chest-sensor system come from Wodicka et al. [8] and Suzuki and Nakayama [9]. These models are for air-coupled sensors - essentially stethoscope chestpieces with a microphone attached in place of the tubing used in acoustic stethoscopes. Wodicka et al. [8] present an acoustic impedance analogy circuit for the combined system using a simple series model for the chest impedance, a two-port model for the air cavity and a series-impedance model for the microphone end load. Their model fulfils its aim of matching the experimentally observed trend due to the variation of one design parameter. However, it does not capture all of the essential features of the coupled system and does not lead to a validated theory for the acoustics of the chest-stethoscope system. Suzuki and Nakayama [9] present two (conflicting) models, both of which are able to match different observed trends, but neither of which paint an accurate picture of the physics of the system.

In this paper we present an approach to modelling the complete coupled system by carefully taking into account the coupling between the chest, the body of the sensor and the cavity. The model is validated by a systematic set of experiments, leading to a new theory for the acoustics of the stethoscope.

2 METHODS - EXPERIMENTS

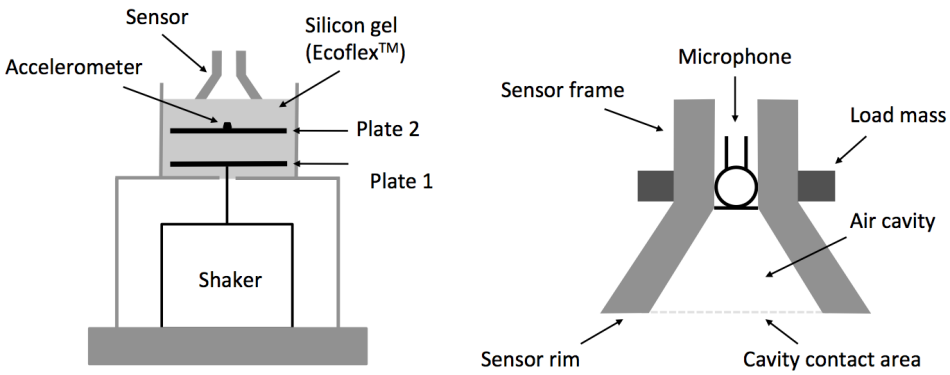

Figure 1. Schematic of 'chest rig' and detail of an air-coupled sensor.

A 'chest phantom' was designed and built in the style of those commonly used in the literature [5][4]. A schematic for the setup is shown in Figure 1. A silicon rubber (Ecoflex™ - density 1.07 kg/l and elastic modulus 69 kPa) was used to replicate the viscoelastic properties of chest tissue. The silicon rubber was cast in a cylindrical perspex tube with an inner diameter of 90 mm. Two rigid plates were embedded in the silicon

rubber. The first plate, at the base of the phantom, was connected to the shaker while the second plate was embedded at an intermediate depth. A piezoelectric accelerometer (PCB M353B15) was attached to the second plate to obtain a reference input signal for computing the air-coupled sensor response.

Stethoscope chest pieces were 3D-printed in Objet VeroWhitePlus RGD835 on an Objet24 3D printer to a variety of geometric specifications to allow the effect of various design parameters on the acoustic response to be investigated. The sensor cavity was terminated by a 1/4 inch microphone (G.R.A.S. 46BL) in each case. A range of masses were applied to the sensor to mimic differences in application pressure. The combined mass of the sensor, microphone and load mass was measured in each case.

An NI cDAQ-9174 chassis with an NI 9234 input module and an NI 9263 output module were used for data acquisition, with MATLAB used as the interface software. The input signal used was a series of chirps over the desired frequency range (5 Hz to 2500 Hz). Signal to noise ratio was high, and averaging over many Fast Fourier Transforms gave smooth (Cross-) Power Spectral Density estimates with minimal noise.

3 METHODS - MODEL

The highest frequency of interest in auscultation is debated but is typically below 3 kHz for most applications [7]. At these frequencies the wavelength of sound (in both the chest tissue and the air cavity) is much larger than the spatial dimensions of the sensor (excluding tubing). Therefore, a lumped element formulation can be used [8]. Two models are presented in this paper. The first is for an 'air-coupled microphone' which is a microphone coupled to the chest via a small air cavity. The second model is for a traditional acoustic stethoscope - again the chest is coupled to a small air cavity, but in this case the cavity is connected to tubing and the ears of the clinician.

3.1 Air-Coupled Microphone Sensor

A model for the air-coupled microphone (see Figure 1) needs to encompass the constitutive properties of the underlying material, the interaction between the rim of the sensor and the material, the motion of the material surface within the cavity and the effect of the compliance of the air cavity.

Kaniusas [6] suggests that the chest surface within the bell acts as a 'natural diaphragm' vibrating in its first mode, which is pre-stressed by the static load from the sensor. However, the assumption that surface tension plays the dominant role in dictating the behaviour of the chest surface within the cavity is not necessarily valid. It is, however, possible to reduce the relation between the rim motion and the interior free surface to a single degree of freedom lumped element model, provided there is only one dominant mode in the frequency range of interest.

Figure 2 shows a simplified mechanical model for the chest-sensor system. In this model x_1 represents an internal displacement (defined at a chosen depth) while x_2 represents the average displacement of the skin surface within the bell. x_2 is linked to x_1 by a constitutive model for the chest medium. For the constitutive model of the chest an inerter (see Smith [10]) is used in parallel with a standard Kelvin-Voigt model to account for kinetic energy of the chest - which will be largely associated with out-of-plane vibration of the medium (due to low compressibility).

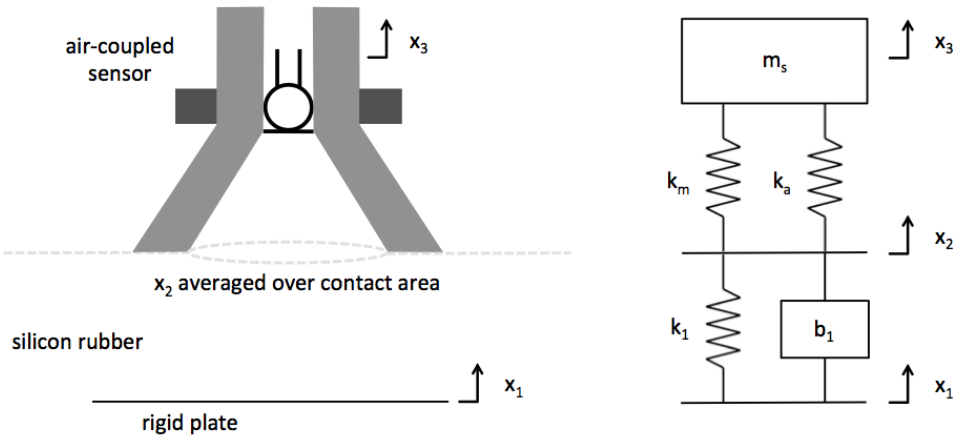

Figure 2. Air-coupled sensor schematic with displacements defined, and a lumped element model for chest-sensor system. Dashpots in parallel with springs have been omitted from the schematic for ease of interpretation but should be included in the analysis.

The displacement of the sensor (mass m_s) is represented by x_3. The skin surface moves with the sensor at the rim, while the surface within the cavity is linked to this motion by the stiffness of the material. In the lumped element model this is represented by the term k_m. The skin surface and the sensor are further related by the stiffness of the air-cavity (k_a). The small size of the cavity with respect to the wavelength of interest means that it can be assumed to be at uniform pressure. The mechanical stiffness of the cavity can thus be calculated as:

$$k_a = \rho c_0^2 A_c^2 \,/\, V \tag{1}$$

where A_c is the contact area between the cavity and the 'skin', ρ is the density of air, c_0^2 is the speed of sound in the cavity and V is the volume of the cavity. Note that at the frequencies of interest it is a fairly good assumption that the microphone can be taken as an infinite impedance, and a 'perfect' measurement of the pressure within the chamber.

The discrete system in Figure 2 can be modelled in matrix form by assuming time-harmonic motion and excitation in the usual manner. This leads to:

$$\mathbf{Ax} = \mathbf{f} \tag{2}$$

where $\mathbf{A}$ is a 3×3 matrix capturing the mass, stiffness and damping terms, $\mathbf{x}$ is a vector of the displacements and $\mathbf{f}$ is a vector of the corresponding forces. For the freely vibrating system, the only term in $\mathbf{f}$ is the input force f_1 applied at x_1. The matrix equation can be solved to express $x_2 - x_3$ in terms of $\ddot{x}_1$ or f_1 as required. The pressure in the cavity is then given by:

$$p_{\text{cavity}} = k_a(x_2 - x_3) \,/\, A_c \tag{3}$$

where it should be noted that x_2 is the displacement of the chest surface averaged over the cavity, such that $A_c(x_2 - x_3)$ is a change in cavity volume.

3.2 Stethoscope

In order to extend the analysis to include acoustical elements, such as the tubing of the stethoscope, an acoustic impedance electrical analogy circuit can be formulated (see e.g. Beranek and Mellow [11]).

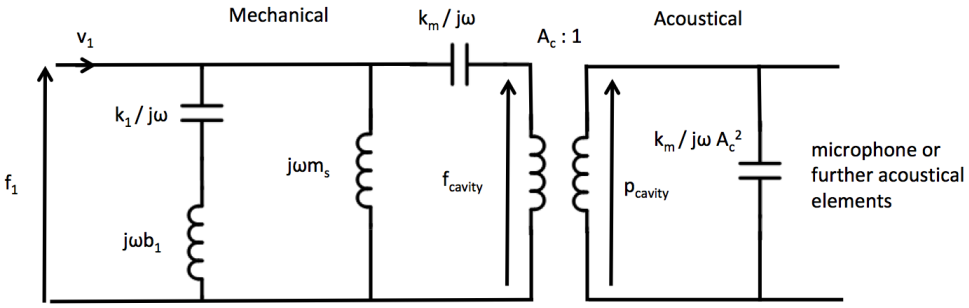

Figure 3. Mechanical impedance analogy for the chest sensor system, coupled to the acoustical impedance analogy circuit for the cavity by a transformer with area ratio A_c. Note that $v_1 = \dot{x}_1$.

The left side of Figure 3 shows a mechanical impedance analogy equivalent circuit of the lumped element model in Figure 2. By using a transformer to represent the interface between the mechanical and acoustical systems it is possible to then add further acoustical elements to the equivalent circuit as shown on the right side of Figure 3.

The length of the tubing in an acoustic stethoscope means that it does not satisfy the condition for lumped element analysis, and thus it must be included as a transmission line in the equivalent circuit. This is shown in Figure 4 which also has the mechanical terms brought to the acoustical side of the transformer by applying the appropriate scaling factors. The entire circuit is now an acoustical impedance analogy circuit with pressure as the 'voltage' and volume velocity as the 'current'. The end load in Figure 4 is an open circuit. In the impedance analogy an open circuit represents a rigid (infinite impedance) termination which is a reasonable approximation given that the impedance of the microphone is very high compared to the other elements in the system. To investigate instead the case where the end load is a human ear a standard ear model can be employed - see e.g. Voss et al. [12].

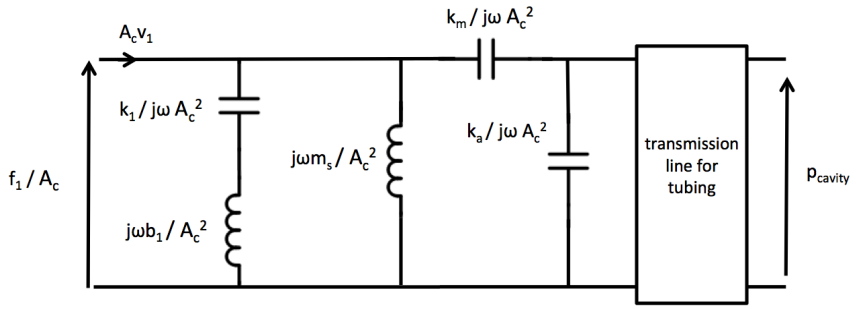

Figure 4. Acoustical impedance analogy equivalent circuit for the complete chest-sensor system including tubing.

A transmission matrix formulation can be employed to link the pressure at the microphone to the pressure and volume velocity terms at the input (see e.g. Beranek and Mellow [11]). For validation against the experimental data obtained in this study the response of the microphone pressure with respect to $\ddot{x}_1$ is computed using MATLAB (R2018b).

4 RESULTS

Figure 5 shows the experimental frequency response function (FRF) for the pressure in the cavity with respect to the acceleration of the embedded base plate within the phantom rig. Several interesting features can be observed in the experimental FRF. There is a low frequency resonance at around 40 Hz, followed by a -40 dB/decade roll off. There is then an anti-resonance at around 400 Hz, followed by a jump in magnitude and a subsequent further region of -40 dB/decade roll off. The jump in response after the anti-resonance is characteristic of a mass shedding effect. These features are of course specific to the rig-sensor combination used, by setting the component values in the model to match this scenario the modelling approach can be validated.

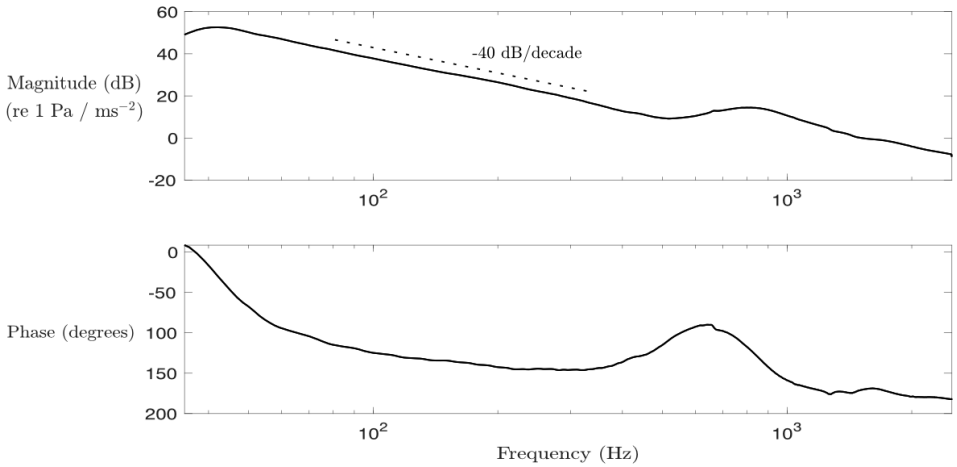

Figure 5. Frequency response function of microphone pressure with respect to base acceleration for an air-coupled microphone with a contact area of 200 mm^2, a cavity volume of 1200 mm^2 and a combined sensor mass of 215 g. Spectrum averaged over 1240 FFTs with a Hann window, 50% overlap and a frequency resolution of 1.6 Hz. Magnitude is expressed in decibels relative to 1 Pa/ms^{-2}.

Figure 6 shows a simulation of the FRF for the same sensor geometry and load mass which was computed using the model described in this paper. Model parameters were estimated for the phantom rig. The fit between the experimental data and the model is good, however, there are discrepancies in the exact shape of the response. These discrepancies arise from two main sources: the estimation of parameter values for the constitutive model of the phantom rig was fairly crude, and furthermore, a lumped element model can never fully describe the behaviour of a continuous system. At higher frequencies (beyond those shown here) higher order modes of the physical system come into play and significantly complicate the response. As the range of frequencies used in auscultation is fairly low this does not impact the validity of the model. In the frequency range shown the model captures the low frequency resonance, the gradual drop-off and the anti-resonance observed in the experimental response. Further to capturing features of the response, the model also accurately predicts the effect of changing cavity volume and contact area, thus providing further validation.

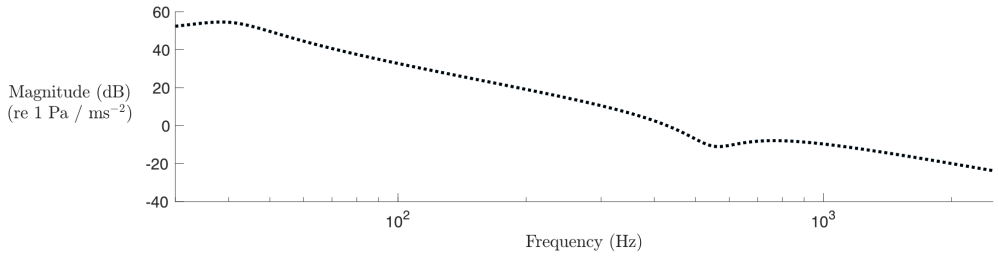

Figure 6. Model Simulation of the frequency response function for cavity pressure (p_{cavity}) with respect to base acceleration ($\ddot{x}_1$) for an air-coupled microphone with the same dimensions and loading as in Figure 5.

The model allows a range of parametric studies to be carried out far more efficiently than by experiments, allowing a wide design space to be explored. It is found that increasing cavity volume lowers the amplitude response, while increasing cavity area increases the response amplitude. Both changes also shift the resonances of the system. Using the acoustical impedance analogy equivalent circuit it is also possible to study the effect of tubing. In general tubing significantly decreases the baseline response (especially at low frequencies) and adds several standing-wave peaks within the frequency range of interest for auscultation. The result is that the frequency profile of lung sounds heard by a physician using an acoustic stethoscope can be very different to that measured at the chest.

5 CONCLUSIONS

We have introduced a new approach to modelling the stethoscope motivated by a careful consideration of the mechanical and acoustical coupling between the chest and the sensor. We have validated our model against a systematic set of experiments carried out on a 'phantom-rig'. The model was able to capture the key features of the frequency response, but further work is needed to adapt the model to the human chest and re-validate it in this setting.

Plotting the response of cavity pressure to the acceleration at a defined depth within the phantom rig is useful for comparison with experimental results, however, as there is no single origin for biological chest sounds, the frequency response to excitation at a single fixed point within the chest is not ultimately the quantity of interest.

It is more interesting to consider how the stethoscope responds to vibrations that have reached the chest surface. The issue here is that the loading of the stethoscope affects the amplitude and properties of the vibrations at the surface. As such, a general reference that is independent of loading is required. There are two options here. One is to use the unloaded 'free-surface' vibration, and the other (suggested by Suzuki [9]) is to use the 'stop-surface' pressure. Neither of these can be easily measured experimentally. However, when using a validated acoustical impedance analogy equivalent circuit it is straightforward to compute the sensor response as a function of one of these references, thus opening up the possibility of a more objective method of classifying sensor performance.

While previous work in the literature has already provided simple models for many of the trends observed between design parameters and acoustic response, this paper goes a step further by introducing a methodology for modelling the complete system, which is not only able to capture these trends independently, but can also provide quantitative predictions and be used to compare designs with several design parameters varied. This allows the model to be used for design optimisation which is an area for future work. In order to optimise the design of an acoustic stethoscope it is further necessary to consider the characteristics of the biological sounds of interest, external noise sources and the selective hearing of the human user.

ACKNOWLEDGEMENTS

The authors would like to thank Dr Ole Nielsen for his advice on lumped element modelling of mechanical and acousitcal systems and for key insights in the modelling approach, Professor Jim Woodhouse for his advice on vibration analysis, Mr John Hazelwood for assistance in the laboratory, Mr Anthony Luckett for CAD work and the 3D printing of sensors, and the Engineering and Physical Sciences Research Council for funding this work.

REFERENCES

[1] Abella, M.; Formolo, J.; Penney, D. G. Comparison of the acoustic properties of six popular stethoscopes. The Journal of the Acoustical Society of America, Vol 91 (4), 1992, pp 2224-2228.

[2] Pasterkamp, H.; Kraman, S. S.; DeFrain, P. D.; Wodicka, G. R. Measurement of respiratory acoustical signals: comparison of sensors. Chest, Vol 104 (5), 1993, pp 1518-1526.

[3] Novak, L.; Novak, K. Discovering new facts and revealing existing myths about the acoustic stethoscope 200 years after its invention, Proceedings of 22nd International Congress on Acoustics, Buenos Aires, Argentina, 5-9 September, 2016, Online.

[4] Mansy, H. A.; Grahe, J.; Royston, T. J.; Sandler, R. H. Investigating a compact phantom and setup for testing body sound transducers, Computers in Biology and Medicine, Vol 41 (6), 2011, pp 361-366.

[5] Kraman, S. S.; Pressler, G. A.; Pasterkamp, H.; Wodicka, G. R. Design, construction, and evaluation of a bioacoustic transducer testing (BATT) system for respiratory sounds. IEEE Transactions on Biomedical Engineering, Vol 53 (8), 2006, pp 1711-1715.

[6] Kaniusas, E. Sensing by Acoustic Biosignals. In Biomedical Signals and Sensors II, Springer, Berlin - Heidelberg, Germany, 1st edition, 2015.

[7] Ertel, P. Y.; Lawrence, M.; Song, W. Stethoscope Acoustics and the Engineer: Concepts and Problems, Journal of the Audio Engineering Society, Vol 19 (3), 1971, 182-186.

[8] Wodicka, G. R.; Kraman, S. S.; Zenk, G. M.; Pasterkamp, H. Measurement of respiratory acoustic signals: effect of microphone air cavity depth, Chest, Vol 106 (4), 1994, pp 1140-1144.

[9] Suzuki, A.; Nakayama, K. Characteristics of lung-sound transducers on chest wall, Japanese Journal of Medical Electronics and Biological Engineering, Vol 38 (4), 2000, pp 298-308.

[10] Smith, M. C. Synthesis of mechanical networks: the inerter. IEEE Transactions on Automatic Control, Vol 47 (10), 2002, 1648-1662.

[11] Beranek, L.; Mellow, T. Acoustics: Sound Fields, Transducers and Vibration. Academic Press, Oxford, UK, 1st edition, 2019.

[12] Voss, S. E.; Rosowski, J. J.; Merchant, S. N.; Peake, W. T. Acoustic responses of the human middle ear. Hearing Research, Vol 150 (1-2), 2000, pp 43-69.